Proceedings of Engineering & Technology PET -Vol 98, pp.7-13 **Advances in Control Systems and Information Technology**

Control of an Electrodynamically Levitated Microgravity Platform

Zehra KARTAL [#1], Kadir ERKAN [*2]

Mechatronics Engineering, Yildiz Technical University
Barbaros Boulevard 34349
Yildiz-İstanbul, Türkiye

Email 1 - zehra.kartal@yildiz.edu.tr
Email 2 - kerkan@yildiz.edu.tr

***Abstract*— This study develops single degree of freedom control of airgap for a microgravity platform based on the principle of induction-based electrodynamic levitation. Using nonlinear levitation force model, relation between disc velocity and airgap is obtained. The nonlinear model of the Halbach array has been linearized using Taylor series expansion and stability analysis are done. Step response of the system examined. PID controller is designed and simulated. To avoid non-minimum phase PI-D and I-PD controllers are designed.**
PID, PI-D, I-PD controllers designed and simulated using MATLAB Simulink. Each controller's control signal and states are exemined. Comparing controller designs performances on system model showed that PID and PI-D controllers result non-minimum phase. As a result, I-PD controller design shows better performance and suitable for using on real time experiments.

***Keywords*— Magnetic levitation, Halbach array, Electrodynamic levitation, Micro-gravity platform, Control**

I. INTRODUCTION

Microgravity platforms are employed to simulate space-like conditions for spacecraft testing. Several methods exist to generate microgravity, including parabolic flights [1], drop towers [2] and air-bed systems [3]. Another approach is electrodynamic levitation, where a moving magnetic field induces thrust over a conductive plate [4]. Electrodynamic levitation can be achieved using specific magnet configurations such as Halbach arrays, in which the magnetization directions are arranged to direct the magnetic flux into a preferred direction. The resulting magnetic field interacts with a conductive plate to generate an electrodynamic force. In this study nonlinear force model is linearized around an operating point and controller design of a microgravity platform with circular Halbach array disc is obtained and simulated using MATLAB Simulink.

II. METHODOLOGY

Micro-gravity platform consists of 4 Halbach array configuration. For one-degree of freedom representation of the system, free-body diagram of Halbach array shown in Fig.1.

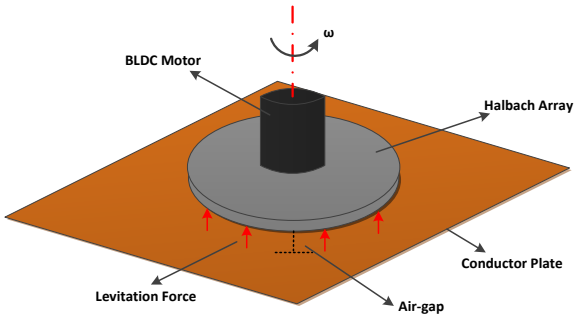

Fig. 1 Free body diagram representation of micro-gravity platform

When the structure of the obtained force model is examined [5],

ISSN: 1737-9334

$$F(z,v) = \frac{N\mu\omega\sigma^2 B_r^2}{2\pi k^3} M^2 \frac{\pi}{M}\left(-e^{-kd}\right)^2 \frac{v^2}{\left(\sqrt{1+\frac{\mu^2\sigma^2v^2}{k^2}}+1\right)^{\frac{3}{2}}\left(\left(\sqrt{1+\frac{\mu^2\sigma^2v^2}{k^2}}+1\right)^{\frac{1}{2}}+\sqrt{2}\right)} e^{-2kz} \quad (1)$$

There exists a nonlinear relationship with variables such as velocity (v) and air gap (z). It is assumed that the designed system operates around a specific operating point. Such expressions can be approximated as linear using a Taylor series expansion about a given operating point (v_0, z_0) [6].

$$F(v,z) \approx F(v_0,z_0) + \frac{\partial F}{\partial v}|_{v_0,z_0}(v-v_0) + \frac{\partial F}{\partial z}|_{v_0,z_0}(z-z_0) \quad (2)$$

Small perturbations around the linearized model of the system,

$$F\big(v(t),z(t)\big) = F((v_0-\Delta v(t),(z_0-\Delta z(t)) = F_z((v_0,z_0)+K_V\,\Delta v(t)+K_z\,\Delta z(t) \quad (3)$$

are expressed accordingly. Determining the analytical values of the K_v and K_z parameters is difficult and time-consuming; therefore, they are computed numerically using MATLAB. The load acting on each disk is calculated as 8.16 kg, and the required force to balance this load at a given air gap is determined as 80.0202 N. Using the analytical model, the velocity required to achieve this force at the selected equilibrium air gap of 0.02 m is then computed. Accordingly, the linearization point of the analytical model is defined as follows:

$$v_0 = 2426\,rpm\,, \qquad z_0 = 0.02\,m$$

The partial derivatives of the levitation force given in Equation 2 with respect to disk speed and air gap are obtained using algorithms implemented in MATLAB. Based on these, the linearized levitation force at the equilibrium point is expressed as follows:

$$F\big(v(t),z(t)\big) = 197.7 + 0.6443\,\Delta v(t) - 6488\,\Delta z(t) \quad (4)$$

It has been observed that the linear model can be utilized within the air gap range of 0.018–0.022 m, defined as the operating interval. Using the linear model, the equation of motion for a single disk is formulated.

$$\mathrm{mz} = \mathrm{F(z,v)} - \mathrm{mg} = 197.7 + 0.6443\,\Delta\mathrm{vt} - 6488\,\Delta\mathrm{zt} - 80.0202 \quad (5)$$

By applying the Laplace transform to the model given in Equation 5, the transfer function of the system corresponding to a single disk is obtained.

$$G(s) = \frac{0.07899}{s^2 + 795.4027} \quad (6)$$

First, the system was analyzed and the model was examined.

$$G(s) = \frac{0.07899}{s^2 + 795.4027}\ , Charasteristic\ equation = s^2 + 795.4027 \quad (7)$$

Then system poles,

$$p_1 = 0.0000 + 28.2029\mathrm{i} \quad p_2 = 0.0000 - 28.2029\mathrm{i}$$

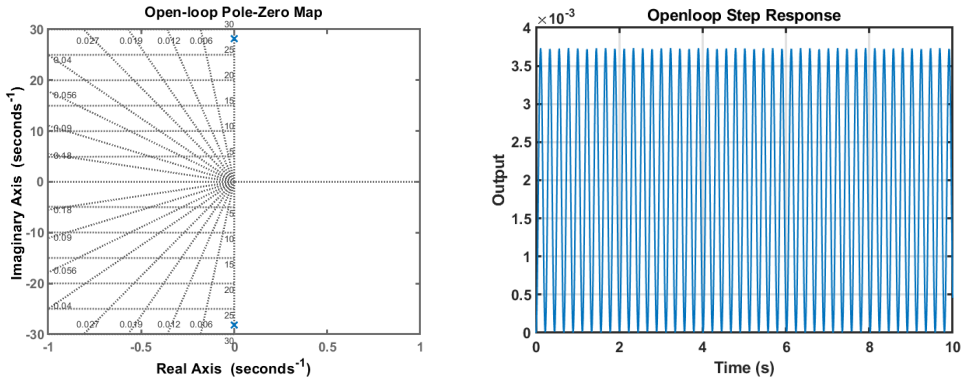

Fig. 2 Open-loop pole-zero map and openloop step response for v=2426 rpm

ISSN: 1737-9334

Using the transfer function, the system poles and the root locus were obtained, and it was observed that the system model has two poles on the imaginary axis (Fig. 2). This indicates that the system is marginally stable [7],[8]. In this case, the system is expected to exhibit oscillations around a certain value.

Using MATLAB, the system response at the equilibrium point was obtained, and marginally stable behavior was observed (Fig. 1). The derived transfer function was then used for the development of control algorithms. For the design of the PID controller, the pole placement method was selected. By incorporating the PID controller into the system structure, a new transfer function $G_{PID}(s)$ was obtained.

$$G_{PID}(s) = \frac{(K_d s + K_p + \frac{K_i}{s})0.07899}{s^2 + 795.4027} \quad 8$$

Then closed-loop transfer function,

$$T_{PID}(s) = \frac{G_{PID}(s)}{1 + G_{PID}(s)} = \frac{(K_d s^2 + K_p s + K_i)0.07899}{s^3 + 0.07899K_d s^2 + (795.4027 + 0.07899K_p)s + 0.07899K_i} \quad 9$$

With the inclusion of the controller structure, the resulting system becomes third order. Initially, a second-order transfer function structure was used to represent the desired system characteristics.

$$\frac{{w_n}^2}{s^2 + 2\zeta w_n s + {w_n}^2} \quad 10$$

Accordingly, the overshoot and settling time were specified for the system response $\%OS = 5 \quad T_s = 0.5s$

Using the specified parameters, the damping ratio and natural frequency corresponding to the desired system characteristics were calculated.

$$\zeta = \frac{\ln 0.05}{\sqrt{\pi^2 + \ln^2 0.05}} = 0.6901 \quad 11$$

$$w_n = \frac{4}{\zeta T_s} = 11.5924 \quad 12$$

The system is third order. Therefore, the third pole to be assigned was selected as three times the natural frequency.

$$p_3 = 3w_n = 34.7772 \quad 13$$

Then characteristic equation,

$$Q_i = (s^2 + 2\zeta w_n s + {w_n}^2)(s + p_3) = s^3 + (2\zeta w_n + p_3)s^2 + (2\zeta w_n p_3 + {w_n}^2)s + {w_n}^2 p_3 \quad 14$$

When these two characteristic equations are equated,

$$s^3 + 0.07899K_d s^2 + (795.4027 + 0.07899K_p)s + 0.07899K_i = s^3 + (2\zeta w_n + p_3)s^2 + (2\zeta w_n p_3 + {w_n}^2)s + {w_n}^2 p_3 \quad 15$$

By substituting the system parameters calculated using the design criteria into the equation, the PID coefficients are obtained.

$$K_p = -1324 \;\; K_i = 59168 \;\; K_d = 642.8525$$

III. Result and Discussion

Designed controller simulated using MATLAB/Simulink and block diagram is given in Fig. 3.

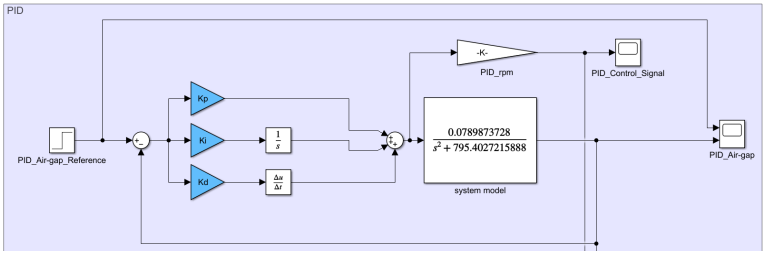

Fig. 3 PID controller block diagram

ISSN: 1737-9334

For small perturbations around the equilibrium point, simulation studies were carried out in MATLAB Simulink by applying a 1 mm air-gap step reference at $t = 1$s (Fig. 4).

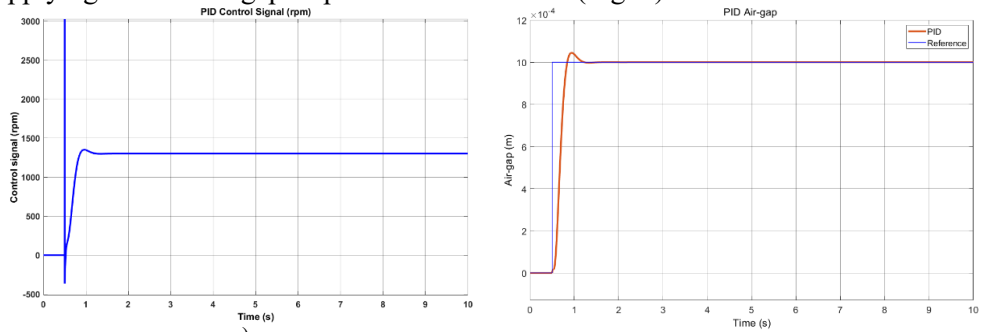

a) b)

Fig. 4 a) PID control signal b) PID air-gap (m)

As a result of the simulation studies, it was observed that the system meets the desired overshoot and settling time specifications for the reference; however, fluctuation occur on reference tracking while control signal has sudden peak at reference change (Fig. 4). Examination of the control signal revealed a momentary large fluctuation that caused by non-minimum phase due to unwanted zero that occurs from PID controller design closed loop transfer function [9]. Derivative kick results as sudden peak caused by taking derivative from error which contains reference step input.

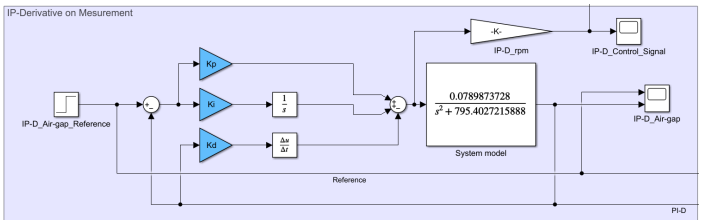

Fig. 5 IP-D block diagram

Accordingly, taking the derivative from the measurement was first investigated which makes the controller become IP-D controller (Fig. 5). This structure is created to eliminate the derivative kick behaviour. With this change in controller, closed loop transfer function does not contain derivative kick, and control signal will not have that large peak at the beginning of reference signal.

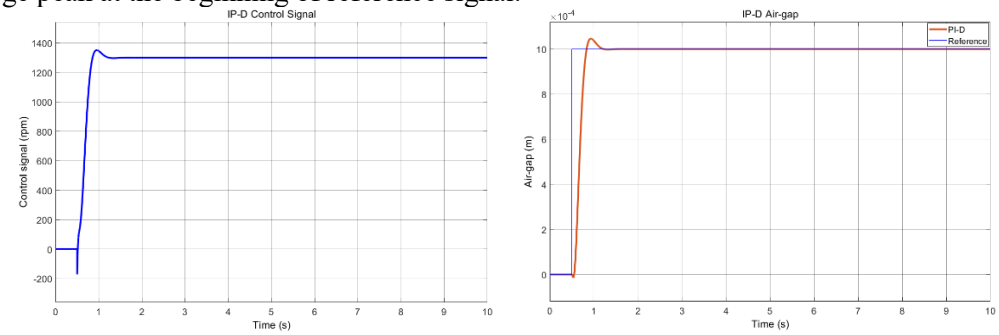

a) b)

Fig. 6 a) IP-D control signal b) IP-D air-gap (m)

When the IP–D controller was applied, an undershoot was observed in the reference tracking (Fig. 6). Examination of the control signal showed that the sudden and large overshoot was eliminated; however, the undershoot remained. This behaviour was attributed to the proportional action that adds system a zero that places on right hand side of imaginary axis, which is called as unwanted zero, leading to the consideration of alternative controller configurations. Due to non-minimum phase behaviour of the system that has unwanted zero, results transient inversion. As a result, undershoot on reference tracking occurs.

ISSN: 1737-9334

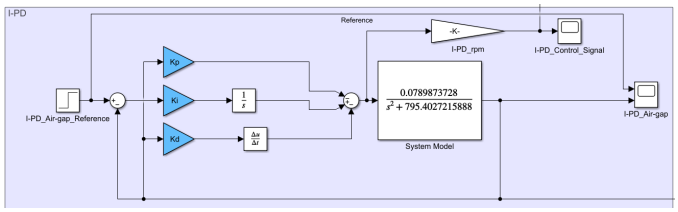

Fig. 7 I-PD control block diagram

To eliminate non-minimum phase behaviour, an I–PD control structure was established by applying the proportional gain and taking the derivative from the measurement feedback (Fig. 7). This structure eliminates the unwanted zero resulting from the proportional gain taken from error signal and derivative kick.

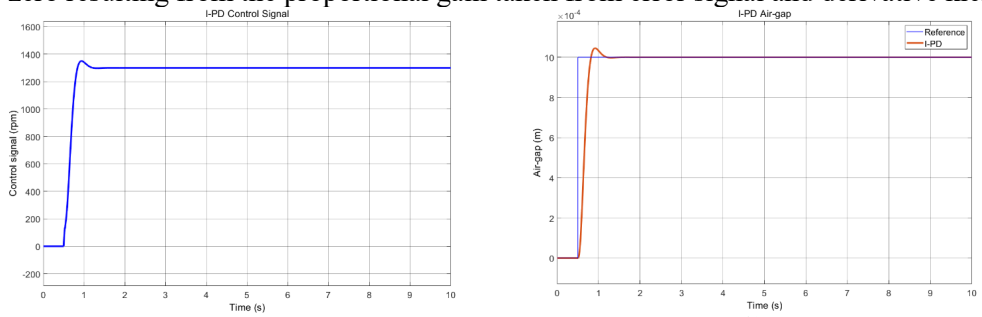

a) b)

Fig. 8 a) I-PD control signal b) I-PD air-gap (m)

When the I–PD control structure was used, it was observed that the system tracks the reference in accordance with the design specifications (Fig. 8). Sudden peak and undershoot caused by non-minimum phase in the control signal were not observed in this controller design. For overall comparison reference tracking response for step response of 0.001 m change in airgap can be seen in Fig. 8. I-PD controller doesn't result with fluctuation or undershoot on airgap response comparing to PID and IP-D controllers. Therefore I-PD controller is choosen for controlling the airgap on real time experiments as a start.

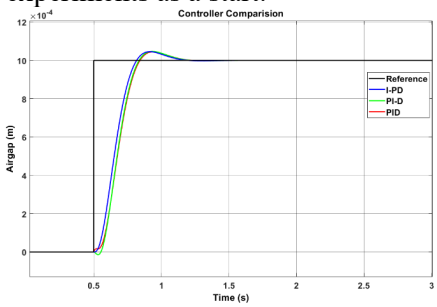

Fig. 9 Controller performance comparison for step response of 0.001 m change in airgap

To observe the behaviour of the designed I–PD controller under the disturbance input F_d, the simulation study shown in Fig. 9 was conducted. Disturbance is taken as 1 newton force to examine response for low disturbance effects. Examining these results, comments about disturbance rejection can be made.

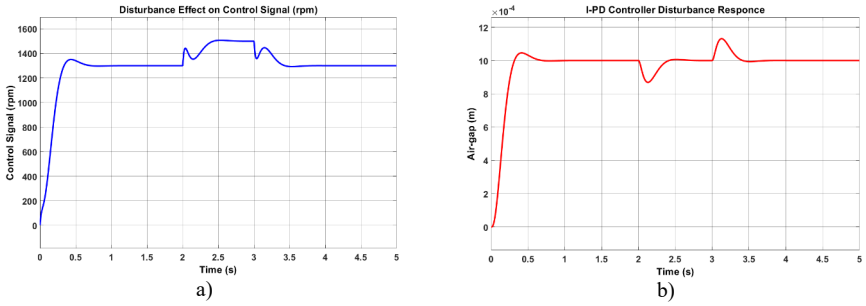

a) b)

Fig. 10 a) Disturbance effect on control signal b) disturbance effect on air-gap response

ISSN: 1737-9334

The control signal generated in response to the applied disturbance input is presented in Fig. 10 a. When the air-gap response is examined (Fig. 9), it can be observed that the designed controller suppresses the disturbance within the settling time specified by the design criteria. However, the simulation results indicates that the disturbance response is slow for such sensitive system.

IV. CONCLUSIONS

This study demonstrates that Halbach array configuration is marginally stable at operating point as revealed by the system analysis that based on linearized force equation. The designed PID controllers' performance was found to be inadequate for this system because of the non-minimum phase that results by derivative on error signal and leads fluctuation on control signal. To address this issue, the derivative term was applied to the feedback path, resulting in an IP-D controller structure. This change in controller resulted with a suppressed control signal but undershoot in control signal remained the same. In the other hand airgap output also resulted with an undershoot. It is seen that I-PD controller eliminates this problem by taking proportional and derivative parts from feedback. I-PD controller resulted in a control signal that did not fluctuate. Controller is able to track reference signal within desired conditions and can suppress the disturbance.

However, despite these improvements, the disturbance response performance of the I-PD controller was observed to be relatively slow, specially for a highly sensitive system such as a microgravity platform that works with a small airgap. Faster and more robust disturbance rejection is necessary in such systems, where the nominal air gap is approximately 2 cm and external disturbances due to loading conditions can be significant.

Therefore, to achieve improved performance in both disturbance rejection and transient response, the development of advanced add-on control structure is proposed as future work. These may include robust or nonlinear control approaches such as sliding mode control (SMC) specially designed to the system's characteristics [10]. In addition, real-time experimental studies will be conducted to validate the simulation results obtained from MATLAB/Simulink for each controller design and to evaluate their practical applicability under realistic operating conditions.

ACKNOWLEDGMENT

This work is supported by the TÜBİTAK as part of the TÜBİTAK 1001 Program under Grant No. 124M098.

REFERENCES

[1] A. Roman-Gonzalez and N. I. Vargas-Cuentas, *Adaptation of a Peruvian Air Force aircraft for parabolic flights: A proposal for microgravity research and training*, presented at the International Astronautical Congress (IAC 2025), Sydney, Australia, Oct. 2025.

[2] Y. Kubo, T. Ando, H. Kawahara, S. Miyata, N. Uchiyama, K. Ito, and Y. Sugawara, *Model evaluation of a transformable CubeSat for nonholonomic attitude reorientation using a drop tower*, arXiv:2501.17173, 2025. [Online]. Available: https://arxiv.org/abs/2501.17173

[3] H. Luo, N. Zhou, H. Zhang, K. Han, N. Zhao, Z. Yang, J. Qi, S. Zhao, J. Zhao, and Y. Zhu, *A microgravity simulation experimental platform for small space robots in orbit*, arXiv:2504.18842, 2025. [Online]. Available: https://arxiv.org/abs/2504.18842

[4] H. Mollahasanoglu, M. Abdioglu, U. K. Ozturk, H. I. Okumus, E. Coskun, and A. Gencer, "Numerical Investigation of EDS Maglev Systems in Terms of Performance and Cost for Different PMs-Aluminum Rail Arrangements," *Journal of Superconductivity and Novel Magnetism*, vol. 38, p. 52, 2025.

[5] Y. Hu, Y. Xu, Z. Long, and Z. Wang, "Control-oriented modeling for the electrodynamic levitation with permanent magnet Halbach array," *International Journal of Applied Electromagnetics and Mechanics*, vol. 68, no. 4, pp. 533–547, 2022.

[6] R. V. Dukkipati, *Vehicle Dynamics*. New Delhi, India: Narosa Publishing House, 2000.

[7] Lendek and C. M. Apostoaia, "Investigation of an electrodynamic magnetic levitation device," in *Proc. IEEE*, Jul. 2020.

[8] Q. Xuesong, S. Qianyuan, S. Zikang, L. Yuhang, and W. Bin, "Analysis of the magnetic levitation characteristics of the vertical Halbach array in a permanent magnet rotor," *Nonlinear Dynamics*, vol. 113, pp. 397–412, 2025.

[9] F. H. Martínez Sarmiento, "Non-minimum phase compensation in quadratic boost converters using PID dual-loop strategies," *World Journal of Advanced Engineering Technology and Sciences*, vol. 16, no. 3, pp. 66–78, 2025.

[10] E. M. Göker, A. F. Bozkurt, and K. Erkan, "Modeling of novel cross-type hybrid 4-pole carrier system and experimental air gap control," *COMPEL - The International Journal for Computation and Mathematics in Electrical and Electronic Engineering*, vol. 43, no. 2, pp. 355–369, 2024.

ISSN: 1737-9334